AGU PUBLICATIONS

JGR

Journal of Geophysical Research: Atmospheres

RESEARCH ARTICLE
10.1002/2015JD024699

Key Points:
- Scale-aware and definition-aware cloud phase evaluation now publicly available in CAM
- When compared to lidar observations, CAM5 has excessive ice cloud and insufficient liquid cloud
- Increasing supercooled liquid cloud reduces shortwave absorption bias, especially over Southern Ocean

Correspondence to:
J. E. Kay,
Jennifer.E.Kay@colorado.edu

Citation:
Kay, J. E., L. Bourdages, N. B. Miller, A. Morrison, V. Yettella, H. Chepfer, and B. Eaton (2016), Evaluating and improving cloud phase in the Community Atmosphere Model version 5 using spaceborne lidar observations, *J. Geophys. Res. Atmos.*, *121*, 4162–4176, doi:10.1002/2015JD024699.

Received 6 JAN 2016
Accepted 4 APR 2016
Accepted article online 8 APR 2016
Published online 25 APR 2016

Evaluating and improving cloud phase in the Community Atmosphere Model version 5 using spaceborne lidar observations

Jennifer E. Kay[1], Line Bourdages[2], Nathaniel B. Miller[1], Ariel Morrison[1], Vineel Yettella[1], Helene Chepfer[3], and Brian Eaton[4]

[1]Cooperative Institute for Research in Environmental Sciences and Department of Atmospheric and Oceanic Sciences, University of Colorado Boulder, Boulder, Colorado, USA, [2]Department of Atmospheric and Oceanic Sciences, McGill University, Montreal, Quebec, Canada, [3]LMD/IPSL, Université Pierre et Marie Curie, Paris, France, [4]National Center for Atmospheric Research, Boulder, Colorado, USA

Abstract Spaceborne lidar observations from the Cloud-Aerosol Lidar and Infrared Pathfinder Satellite Observation (CALIPSO) satellite are used to evaluate cloud amount and cloud phase in the Community Atmosphere Model version 5 (CAM5), the atmospheric component of a widely used state-of-the-art global coupled climate model (Community Earth System Model). By embedding a lidar simulator within CAM5, the idiosyncrasies of spaceborne lidar cloud detection and phase assignment are replicated. As a result, this study makes scale-aware and definition-aware comparisons between model-simulated and observed cloud amount and cloud phase. In the global mean, CAM5 has insufficient liquid cloud and excessive ice cloud when compared to CALIPSO observations. Over the ice-covered Arctic Ocean, CAM5 has insufficient liquid cloud in all seasons. Having important implications for projections of future sea level rise, a liquid cloud deficit contributes to a cold bias of 2–3°C for summer daily maximum near-surface air temperatures at Summit, Greenland. Over the midlatitude storm tracks, CAM5 has excessive ice cloud and insufficient liquid cloud. Storm track cloud phase biases in CAM5 maximize over the Southern Ocean, which also has larger-than-observed seasonal variations in cloud phase. Physical parameter modifications reduce the Southern Ocean cloud phase and shortwave radiation biases in CAM5 and illustrate the power of the CALIPSO observations as an observational constraint. The results also highlight the importance of using a regime-based, as opposed to a geographic-based, model evaluation approach. More generally, the results demonstrate the importance and value of simulator-enabled comparisons of cloud phase in models used for future climate projection.

1. Introduction

Clouds regulate the Earth's energy budget by modifying both the reflection of incoming solar radiation and the emission of infrared radiation. At temperatures well below the melting point, low-level supercooled liquid-containing clouds have an important influence on surface radiative fluxes in polar regions [*Van Tricht et al.*, 2016; *Miller et al.*, 2015; *Shupe and Intrieri*, 2004; *Cesana et al.*, 2012] and midlatitude oceans [*Bodas-Salcedo et al.*, 2014; *Forbes and Ahlgrimm*, 2014; *Kay et al.*, 2014]. The overall influence of low-level supercooled liquid-containing clouds on surface radiative fluxes depends on the incident solar flux and the underlying surface albedo. Over regions with high-surface albedos, longwave cloud radiative forcing dominates and total cloud radiative forcing is generally positive (i.e., clouds warm the surface). For example, clouds over Summit, Greenland, on average warm the surface because the longwave cloud radiative effect is larger than the shortwave cloud radiative effect. While *Van Tricht et al.* [2016] estimate that liquid clouds and ice clouds contribute equally to increasing surface fluxes over Greenland, *Miller et al.* [2015] found the warming magnitude of Greenland clouds closely tracks the occurrence frequency of low-level supercooled liquid-containing clouds. In contrast to Greenland, regions with low-surface albedo and large incident shortwave radiation have large cloud shortwave effects and cloud radiative forcing that is generally negative (i.e., clouds cool the surface). For example, supercooled liquid cloud water in low-level clouds cool the Southern Ocean, a region taking up anthropogenic carbon and heat and thus regulating the pace of global warming [*Frölicher et al.*, 2015; *Mikaloff-Fletcher*, 2015]. Coincident with observed global warming and ice melting [*Stroeve et al.*, 2012; *Shepherd et al.*, 2012], observations have revealed that polar clouds regulate both sea ice loss [e.g., *Kay et al.*, 2008] and ice sheet melt [e.g., *Bennartz et al.*, 2013]. Given the important influence of low-level supercooled

liquid clouds on radiative fluxes, and in turn-on rates of warming and sea level rise in response to increased greenhouse gases, cloud phase is especially important to evaluate in models used for future climate projection.

The presence of supercooled liquid in clouds cannot be predicted by temperature alone [e.g., *Morrison et al*., 2012]. Instead, cloud phase emerges from the complex and incompletely understood cloud microphysical processes and their interactions with the atmospheric circulation. As a result, observations are needed to quantify cloud phase and to evaluate and improve the representation of cloud phase in climate models. Fortunately, reliable global observations of cloud phase have become available in the last decade. Launched in spring 2006, the spaceborne lidar Cloud-Aerosol Lidar with Orthogonal Polarization on board the Cloud-Aerosol Lidar and Infrared Pathfinder Satellite Observation (CALIPSO) satellite [*Winker et al*., 2010] directly measures cloud amount and phase using the backscattered and depolarized returned lidar signal [*Cesana and Chepfer*, 2013; *Hu et al*., 2010]. As such, CALIPSO observations provide a unique global observational constraint on cloud phase and permit evaluation of cloud phase in global climate models [*Cesana et al*., 2012; *Cesana and Chepfer*, 2013].

The goal of this paper is to evaluate cloud phase biases and their impacts on climate simulated within the Community Earth System Model (CESM) [*Hurrell et al*., 2013]. CESM is a publicly available, globally used, state-of-the-art global coupled climate model. To evaluate clouds within the atmospheric component of CESM (Community Atmosphere Model (CAM) version 5 (CAM5)), we use CALIPSO observations and a community satellite simulator package: the Cloud Feedback Model Intercomparison Project (CFMIP) Observational Simulator Package, COSP [*Bodas-Salcedo et al*., 2011]. Previous studies have evaluated CESM clouds using the simulators in COSP [*Kay et al*., 2012; *English et al*., 2014], but evaluation of cloud phase using CALIPSO observations and the influence of cloud phase biases on the simulated climate within CESM is a new contribution of this study.

In this study, we take great care to make scale-aware and definition-aware comparisons between modeled and observed clouds. Using the subcolumn generator in COSP, we account for the differing spatial scales at which climate models simulate clouds (~100 km) and spaceborne lidars observe clouds (~1 km). In other words, we make "scale-aware" comparisons by downscaling the climate model gridbox scale to the much higher-resolution lidar observation scale. Making quantitative comparisons also requires being "definition aware," i.e., using same criteria for cloud detection in the model and the observations. Spatiotemporal averaging, lidar attenuation, and retrieval assumptions all affect spaceborne lidar cloud detection. We account for these lidar idiosyncrasies and therefore can make definition-aware comparisons between model-simulated and lidar-observed clouds.

The scope of this study is global, but we focus on extratropical clouds. We compare observed and modeled Arctic clouds. We also examine both Antarctic and Southern Ocean cloud and cloud phase biases. Finally, we use CALIPSO cloud phase diagnostics to evaluate a recent effort to reduce long-standing shortwave radiation biases via modifications to parameterized processes controlling cloud phase in CAM5. Our results demonstrate the substantial influence of cloud phase biases on simulated climate and provide insights into underlying processes and potential ramifications of cloud phase biases for future climate projection.

2. Methods

2.1. COSP1.4 Implementation in CAM

The instrument simulators contained within COSP version 1.3 have been implemented in CAM versions 4 and 5 [*Kay et al*., 2012]. This paper serves to document the upgrade to COSP version 1.4 in CAM and therefore CESM. COSP1.4 includes new cloud phase diagnostics [*Cesana and Chepfer*, 2013] in the CALIPSO simulator [*Chepfer et al*., 2008]. The COSP1.4 implementation in CAM also retains modifications for radiatively active snow developed specifically for CAM [*Kay et al*., 2012; *English et al*., 2014].

2.2. CAM Experiments

CAM version 5 [*Neale et al*., 2012] is the most recent officially released atmospheric model within CESM. CAM5 was used for Coupled Model Intercomparison Project 5 (CMIP5) [*Taylor et al*., 2012] and also recent climate modeling projects within CESM including the recent CESM Large Ensemble Project [*Kay et al*., 2015]. This paper assesses CAM5 cloud phase biases by comparing 10 year (2003–2012) atmosphere-only runs with prescribed observed sea surface temperatures and sea ice to CALIPSO observations. All model runs use the finite volume dynamical core and are run at ~1° horizontal resolution (0.9×1.25). We analyze CAM5 physics in a development version of the code (CAM tag cam5_3_88). This code base has CAM5 physics consistent with

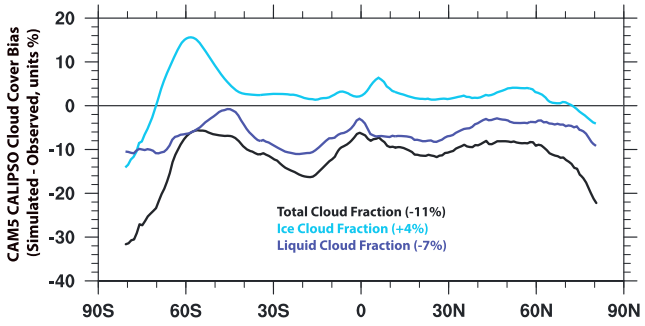

Figure 1. Zonal annual mean CAM5 CALIPSO cloud cover bias (CAM5 simulated − observed, units %). Global mean values are indicated in parenthesis.

CMIP5, but the CAM5 climate is not bit for bit with CMIP5 CAM5 due to bug fixes that have been implemented within the CAM code base. Our comparison with CMIP5 CAM5 and the development CAM5 shows zonal mean CALIPSO total cloud fractions within 2% of CMIP5 CAM5. Cloud fraction differences between CAM5 and CALIPSO observations greatly exceed cloud fraction differences between CAM5 variants (Figure 1 [*Kay et al*., 2012]). To demonstrate the value for evaluation of parameterization changes, we also evaluate a modified version of CAM5 with large reductions in shortwave radiation bias as described in *Kay et al*. [2016]. The model experiments are described in Table 1.

2.3. Observations

We use Global Climate Model (GCM)-Oriented CALIPSO Cloud Product (CALIPSO-GOCCP) [*Chepfer et al*., 2010] version 2.68 for the years 2006–2012. As described in *Chepfer et al*. [2010], CALIPSO-GOCCP has been processed specifically for studies utilizing COSP to make definition-aware and scale-aware comparisons between CALIPSO lidar observations and climate models. CALIPSO-GOCCP total cloud cover maps and cloud fraction profiles have been used to benchmark the cloud amount and the cloud vertical distribution in CMIP5 and CFMIP-2 models [e.g., *Cesana and Chepfer*, 2012; *Kay et al*., 2012; *Nam et al*., 2012; *Bodas-Salcedo et al*., 2014]. CALIPSO-GOCCP retrievals have also been compared to other CALIPSO cloud products [*Chepfer et al*., 2013] and other passive satellite products within the Global Energy and Water Cycle Experiment cloud assessment [*Stubenrauch et al*., 2013]. Due to the CALIPSO instrument sensitivity and CALIPSO-GOCCP retrieval methodologies, CALIPSO-GOCCP products differ from other satellite-based cloud products including other observational products based on CALIPSO level 1 data. It is inevitable to have differences between observational products that define clouds in different ways. In fact, knowing that we expect observational products to differ depending on their cloud detection assumptions underscores the importance of using a definition-aware and scale-aware framework for model-observation comparisons.

CALIPSO-GOCCP splits the atmosphere into cloudy (lidar scattering ratio (SR) > 5), clear (SR < 1.2), fully attenuated (SR < 0.01), and unclassified pixels ($1.2 <$ SR < 5). For reference, a scattering ratio of 5 is common when low-level liquid clouds have cloud optical depth (τ) exceeding 0.1 or cloud liquid water path exceeding 0.1–0.2 gm^{-2} (assuming a cloud thickness 250–500 m and a particle radius of 12 μm) [*Chepfer et al*., 2010]. Fully attenuated pixels typically occur when cloud optical depths (τ) exceed 3–5. The unclassified pixels ($1.2 <$ SR < 5) contain aerosols and possibly optically very thin clouds ($\tau < 0.1$ [*Chepfer et al*., 2013]).

The CALIPSO-GOCCP Cloud Phase product [*Cesana and Chepfer*, 2013] contains maps of liquid, ice, and undefined-phase cloud fraction on a $2 \times 2°$ grid as well as profiles of liquid, ice, and undefined-phase cloud fraction with 480 m vertical resolution. As described in *Cesana and Chepfer* [2013], cloudy pixels are classified as liquid-containing, ice-dominated, or undefined using the polarization state of laser light scattered by cloud particles (multiple scattering is taken into account) and temperature. The temperature criterion is used to

Table 1. Description of Atmosphere-Only Simulations[a]

Name	Length (Years)	Description
CAM5	10, 2003–2012	Atmosphere-only control with CAM5 physics (CAM tag CAM5_3_88)
CAM5*	10, 2003–2012	Atmosphere-only experiment with CAM5 physics (CAM tag CAM5_3_88) and modifications described in *Kay et al.* [2016] to increase supercooled liquid in shallow convective clouds and tune for global radiative balance. All modifications to the code base implemented for CAM5* are provided in the supporting information

[a]All simulations use the Community Atmosphere Model version 5 (CAM5) [*Neale et al*., 2012] at 1° horizontal resolution with the finite volume dynamical core. All simulations use fully prognostic atmosphere and land models with specified observed sea surface temperatures and sea ice extent.

Table 2. Zonal Annual Mean Total, Liquid, and Ice Cloud Cover (CC) in Units of Percent from CALIPSO Observations [*Chepfer et al.*, 2010; *Cesana and Chepfer*, 2013] and CAM5 Bias (CAM5-Observed)[a]

	Observed Total CC (%)	CAM5 Total CC Bias (%)	Observed Liquid CC (%)	CAM5 Liquid CC Bias (%)	Observed Ice CC (%)	CAM5 Ice CC Bias (%)
70–82 N	71	−16	38	−6	22	−1
60–70 N	71	−11	32	−4	26	2
50–60 N	74	−8	34	−4	26	4
40–50 N	67	−8	30	−3	25	3
30–40 N	59	−10	27	−6	22	2
20–30 N	52	−11	27	−8	17	2
10–20 N	58	−10	26	−7	24	3
0–10 N	70	−8	29	−6	31	5
0–10 S	64	−9	29	−6	25	3
10–20 S	60	−15	32	−10	18	2
20–30 S	58	−14	33	−10	14	3
30–40 S	68	−11	38	−8	18	3
40–50 S	81	−7	44	−2	21	5
50–60 S	89	−6	48	−5	23	14
60–70 S	87	−14	44	−9	26	10
70–82 S	61	−27	21	−10	30	−7
Global	67	−11	33	−7	22	4

[a]See Table 1 for CAM5 description.

identify the phase of less than 1% of the identified cloudy cases. *Cesana and Chepfer* [2013] report that ~10% of the clouds identified in the CALIPSO-GOCCP retrieval have a phase classified as undefined. These undefined-phase clouds correspond to cloud layers located directly below relatively high reflecting clouds (i.e., clouds that produce a lidar scattering ratio >30). In these situations, the depolarization signal measured by CALIPSO is attenuated and becomes too noisy to reliably determine cloud phase. We note that many low-level mixed phase are optically thick supercooled liquid clouds that are precipitating snow and would be classified as "liquid" clouds by CALIPSO.

3. Results

3.1. Global Cloud Amount and Cloud Phase

Simulator-enabled comparisons of global annual mean CALIPSO cloud cover show that CAM5 (56%) has insufficient total cloud when compared to CALIPSO-GOCCP observations (67%), consistent with previous studies [*Kay et al.*, 2012]. Illustrating the power of the newly available CALIPSO cloud phase diagnostics, we find insufficient global total cloud cover in CAM5 results in large part because CAM5 has insufficient liquid cloud. Specifically, the CAM5 global annual mean liquid cloud cover (26%) is 7% lower than the observed equivalent (33%). In contrast, CAM5 has excessive ice cloud (26%) when compared to CALIPSO-GOCCP observations (22%). Zonal mean comparisons (Figure 1 and Table 2) reveal that insufficient liquid and excessive ice cloud biases are present throughout the tropics and the midlatitudes, while poleward of ~70° there is both insufficient liquid cloud cover and ice cloud cover in both hemispheres.

Annual mean cloud cover maps show qualitative agreement between the modeled and observed spatial distributions of liquid and ice cloud (Figure 2). In both CAM5 and CALIPSO-GOCCP observations, large liquid cloud cover occurs over the oceanic midlatitude storm tracks and in the subtropics off western continental boundaries. Large ice cloud cover occurs where tropical convection dominates including over the tropical western Pacific, the Amazon, and Africa. Consistent with common rainfall biases in climate models [e.g., *Hwang and Frierson*, 2013], CAM5 has excessive ice cloud in the southern extension of the Intertropical Convergence Zone. Global maps also show excessive ice cloud over the storm tracks in CAM5, especially at southern midlatitudes. Over the Southern Ocean (herein defined as 40–70°S), excessive ice cloud fraction and insufficient liquid cloud fraction biases compensate.

3.2. Arctic Cloud Amount and Cloud Phase

We begin by showing North Pole maps of CALIPSO-observed total Arctic cloud cover. The maps reveal that CALIPSO-observed Arctic cloud distributions vary both geographically and seasonally (Figures 3a–3d). CALIPSO-observed Arctic cloud cover is large (>90%) over the North Atlantic and North Pacific storm tracks

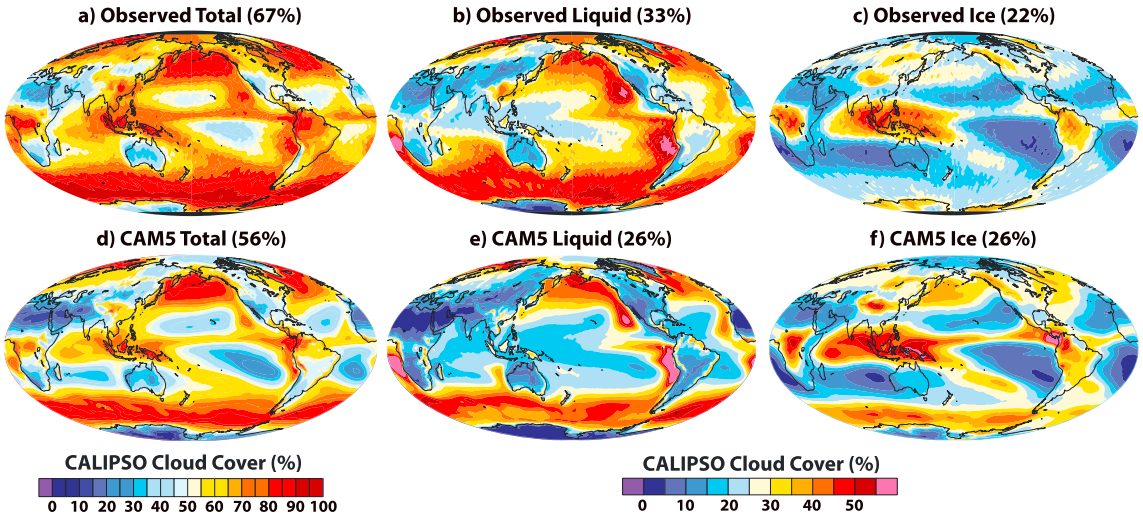

Figure 2. Global maps of CALIPSO cloud cover (units %): (a) observed total, (b) observed liquid, (c) observed ice, (d) CAM5 total, (e) CAM5 liquid, and (f) CAM5 ice. Global mean values are indicated in parenthesis.

and also over the Arctic Ocean during northern hemisphere summer (June-July-August (JJA)) and fall (September-October-November (SON)). In contrast, total cloud cover over the Arctic Ocean is smaller (<70%) during northern hemisphere spring (March-April-May (MAM)) and even smaller (<50%) during northern hemisphere winter (December-January-February (DJF)). In general, Arctic land areas have less

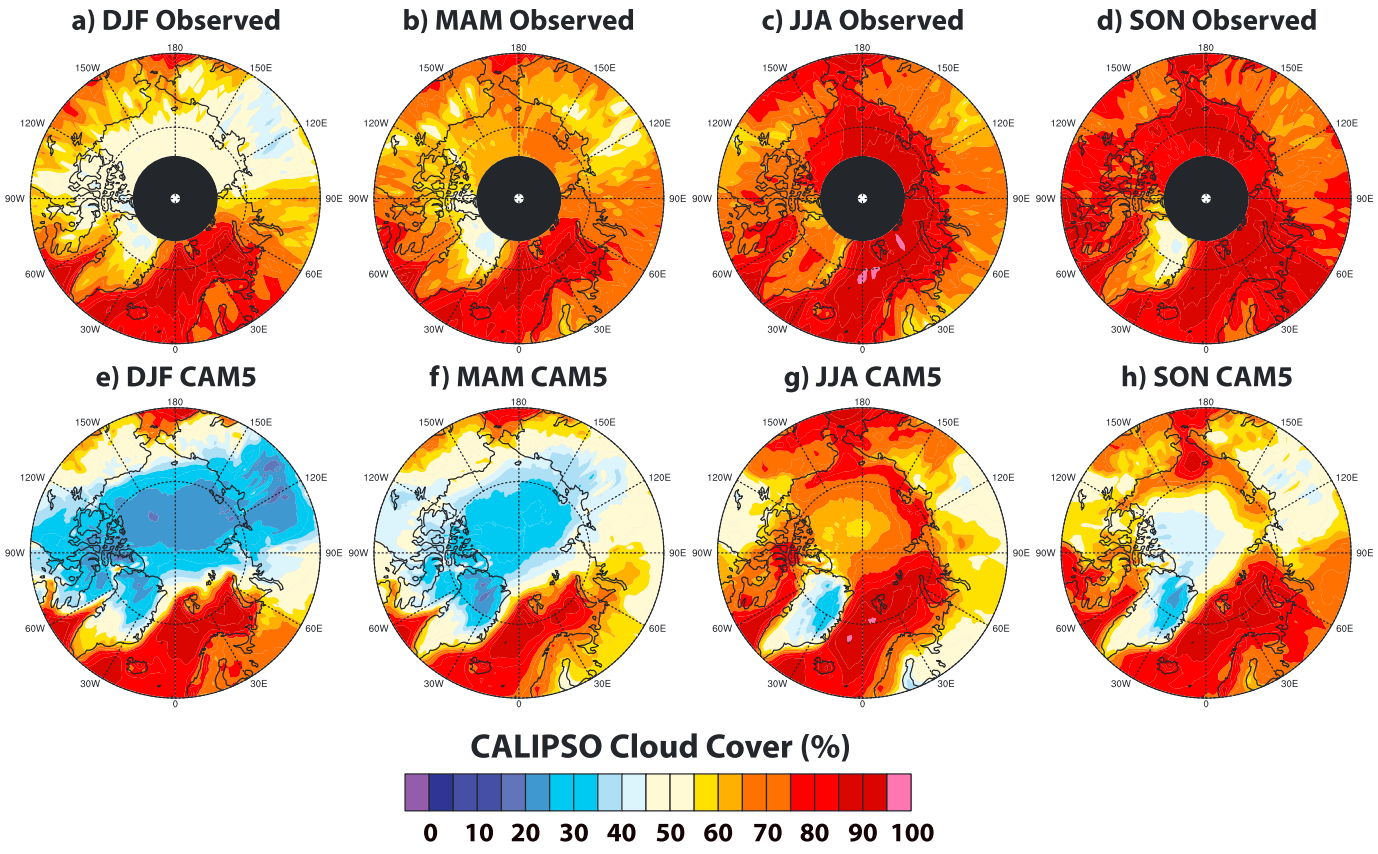

Figure 3. North Pole maps (60–90°N) of total CALIPSO cloud cover (units %) by season: (a) DJF observed, (b) MAM observed, (c) JJA observed, and (d) SON observed. (e–h) Same as in Figures 3a and 3b but for CAM5.

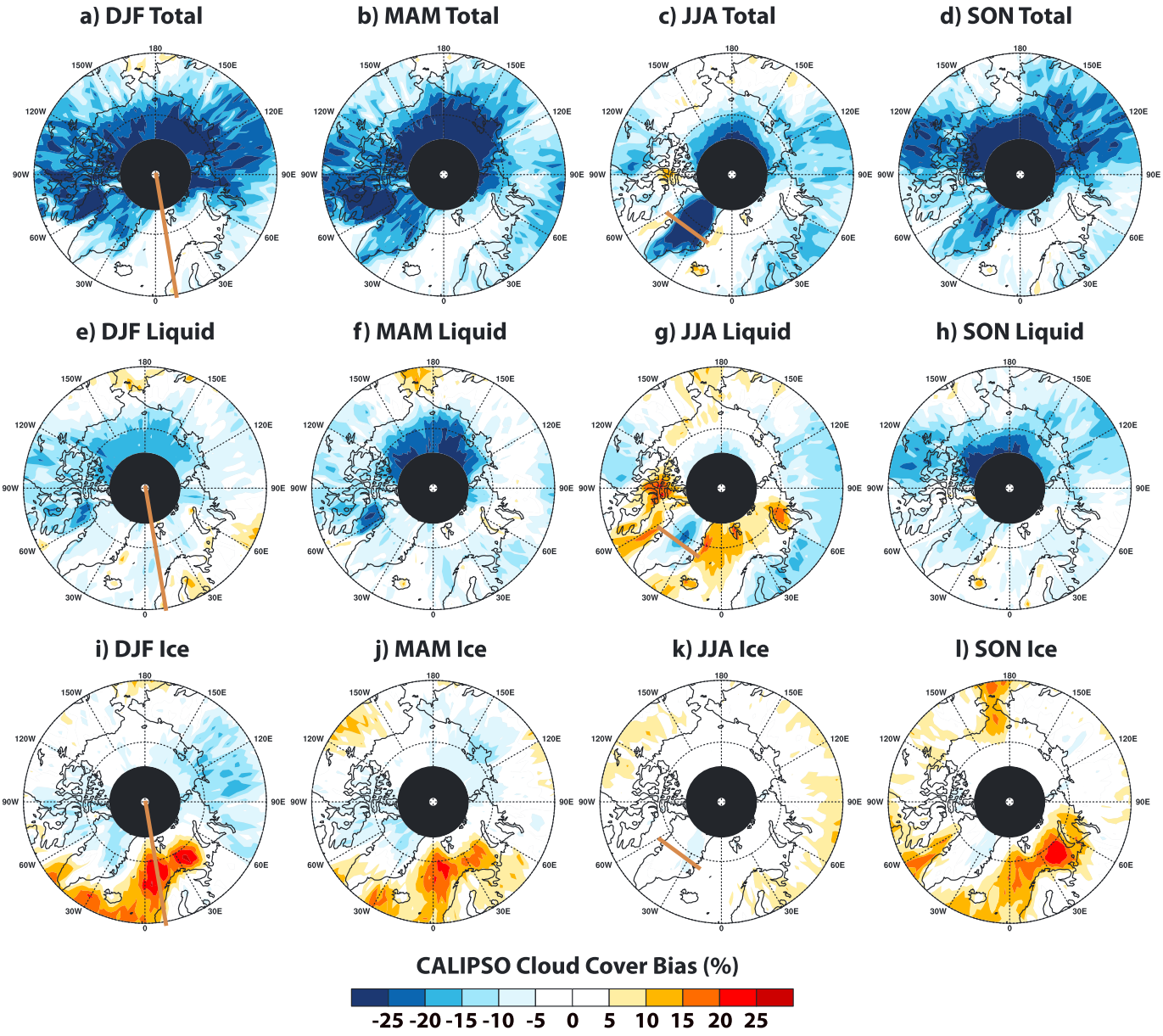

Figure 4. North Pole maps (60–90°N) of CALIPSO cloud cover bias (CAM5 simulated − observed, units %) by season: (a) DJF total, (b) MAM total, (c) JJA total, and (d) SON total. (e–h) Same as in Figures 4a–4d but for liquid cloud cover. (i–l) Same as in Figures 4a–4d but for ice cloud cover. The brown lines indicate the location of the cross section shown in Figures 5a, 5e, and 5i and for Figures 6c, 6g, and 6k.

CALIPSO-observed cloud cover than ocean-covered areas. Total cloud cover is especially small (<55%) during northern hemisphere winter when land and ice-covered areas are isolated from the moistening influence of the North Atlantic and North Pacific storm tracks.

Although CAM5 matches spatial aspects of CALIPSO-observed Arctic cloud distribution including more cloud cover in the storm tracks and less cloud cover over the central Arctic Ocean and Arctic land, CAM5 suffers from substantial Arctic cloud cover biases (Figures 3 and 4a–4d). Over the Arctic Ocean, CAM5 underestimates total cloud cover in all seasons and biases are locally very large (>25%). The very large Arctic Ocean cloud deficits are geographically widespread in SON, MAM, and DJF but concentrated poleward of 75°N in JJA. Over Arctic land areas, CAM5 also underestimates total cloud cover, especially over Greenland in summer (JJA) and over Siberia and central Canada during northern hemisphere fall (SON) and winter (DJF). In contrast to the large total cloud underestimation over the Arctic ocean and land, CAM5 total cloud cover is within 5% of CALIPSO observations over the North Pacific and North Atlantic storm tracks.

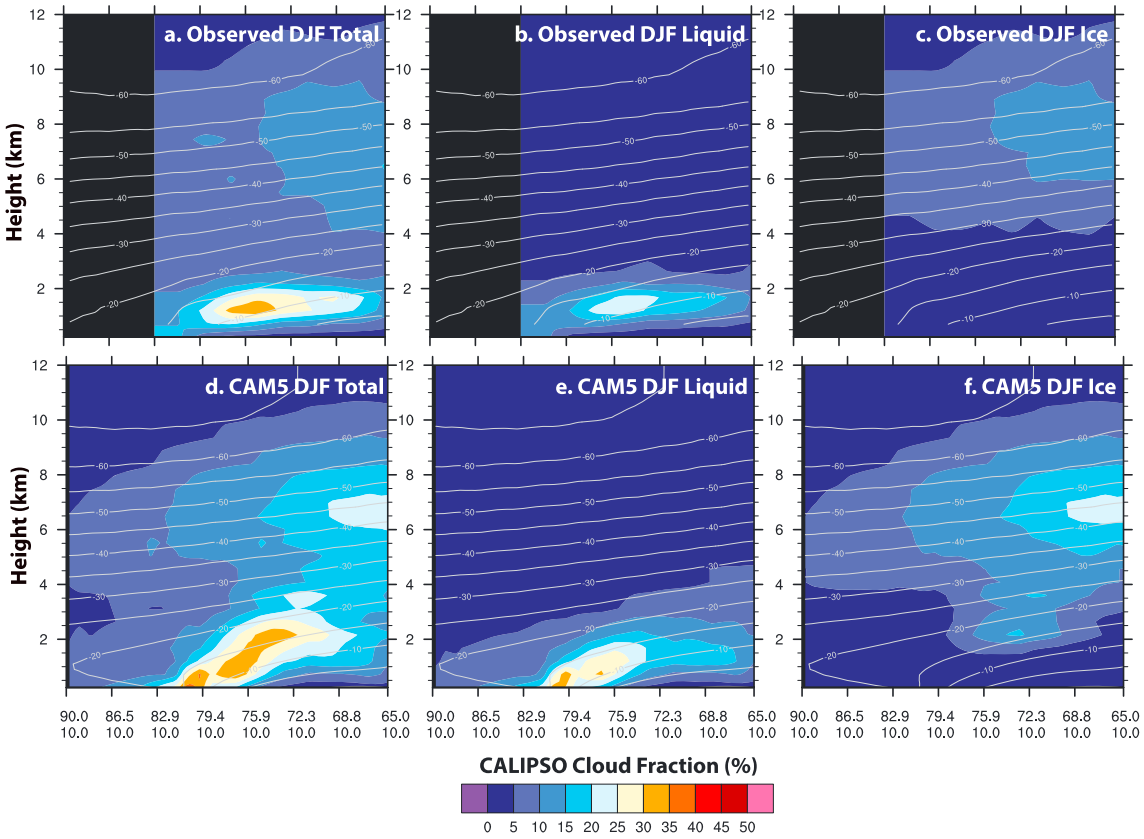

Figure 5. Vertical cross section of CALIPSO clouds and temperatures across the North Atlantic sea ice edge during northern hemisphere winter (DJF): (a) observed total, (b) observed liquid, (c) observed ice, (d) CAM5 simulated total, (e) CAM5 simulated liquid, and (f) CAM5 simulated ice. The contour colors show the CALIPSO cloud fraction (units %), while the grey contour lines show the air temperature (units °C) from ERA-Interim [*Dee et al.*, 2011].

Arctic total cloud biases over the Arctic ocean and land differ from those over the high-latitude oceanic storm tracks. What is the contribution of cloud phase biases to the total cloud cover biases? When compared to spaceborne lidar observations, CAM5 has insufficient liquid cloud cover (Figures 4e–4h) over the Arctic ocean and land, especially in the transition seasons (MAM and SON). In contrast, ice cloud cover biases are small (<5%) over the Arctic ocean and land. Thus, insufficient total cloud cover over the Arctic Ocean in CAM5 is primarily explained by a liquid cloud deficit. Over the high northern latitude storm tracks, the cloud phase biases are opposite in nature. The storm tracks have excessive ice cloud cover (bias >15%) in the North Atlantic during DJF, MAM, and SON and in the North Pacific in SON. Liquid cloud biases are small except during JJA when CAM5 has excessive liquid cloud in the North Atlantic.

Intrigued by excessive ice cloud cover biases over the storm tracks (Figures 4i–4l), we next examine a cross section through the atmosphere of the North Atlantic (Figure 5). The location of the cross section in map view is indicated in Figures 4a, 4e, and 4i. The cross section enables visualization of vertical structure of cloud phase biases discovered in map view and their association with temperature. We present DJF cross sections to evaluate vertical cloud fraction and temperature structures when ice cloud phase biases and storm activity both reach their maximum values. The DJF North Atlantic cross section reveals low-level cold air outbreak clouds forming over open water and middle/high-level clouds formed by frontal lifting within cyclones. The CAM5-simulated clouds trace a more pronounced deepening of the atmospheric boundary layer at the sea ice edge (~75°N) than is implied by CALIPSO observations. In agreement with observations, CAM5 clouds are primarily liquid near the surface (<1.5 km above sea level). But consistent with the bias identified in ice cloud cover maps (Figure 4i), CAM5 has excessive ice cloud over the North Atlantic (Figures 5c and 5f). CAM5 has ice clouds present in the −15 to −25°C temperature range that are not present in the observations. In addition, CAM5 has larger-than-observed ice cloud fractions in the temperature range from −25 to −65°C.

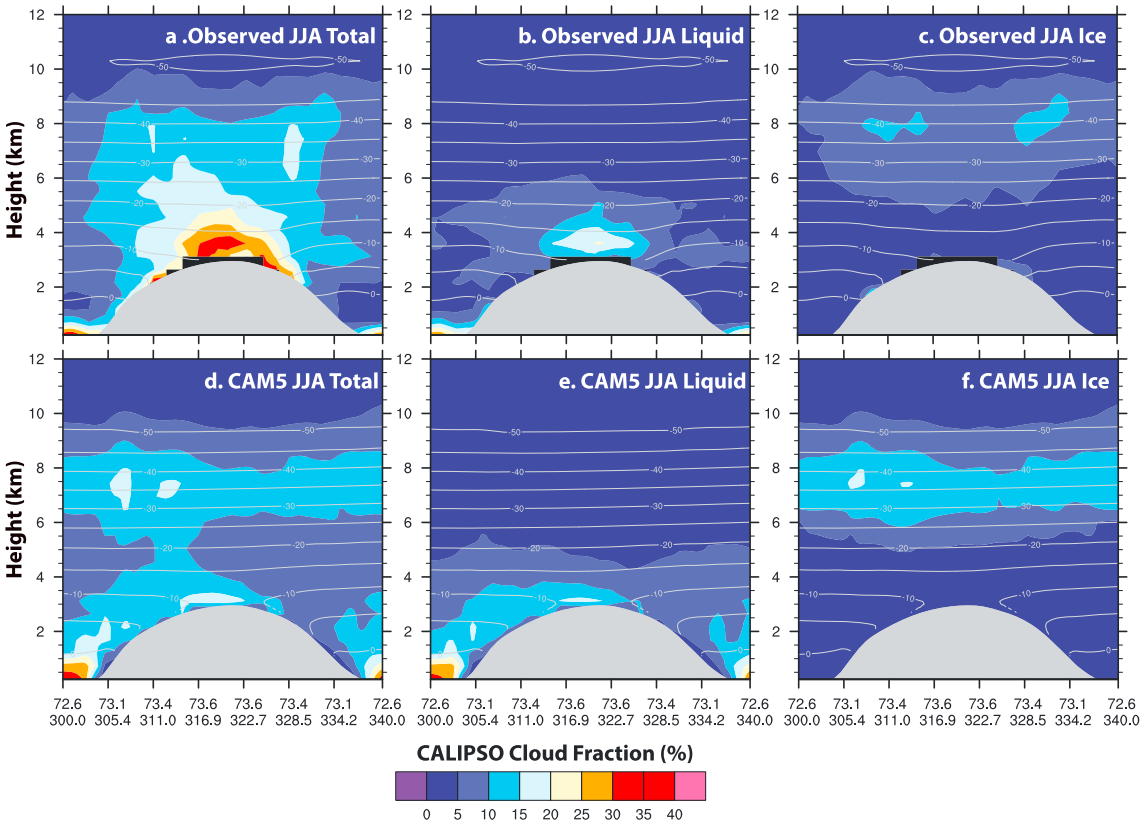

Figure 6. Vertical cross section of CALIPSO clouds and temperatures Greenland during northern hemisphere summer (JJA): (a) observed total, (b) observed liquid, (c) observed ice, (d) CAM5 simulated total, (e) CAM5 simulated liquid, and (f) CAM5 simulated ice. The contour colors show the CALIPSO cloud fraction (units %), while the grey contour lines show the air temperature (units °C) from ERA-Interim [*Dee et al.*, 2011].

Recognizing the importance of clouds over Greenland for melt and global sea level rise, and noting the large total and liquid northern hemisphere summer (JJA) cloud cover biases over Greenland evident in map view (Figures 4c and 4g), we next examine JJA vertical cross sections of cloud fraction above Greenland (Figure 6). Consistent with the bias map, the northern hemisphere summer cross sections reveal insufficient total cloud over central Greenland from the surface to the −20°C isotherm (Figures 6a and 6d). Looking at cloud phase biases shows that the insufficient CAM5 cloud is primarily resulting from insufficient liquid clouds (Figures 6b and 6e). While CALIPSO does observe more liquid cloud than CAM5 simulates, the sum of the liquid clouds (Figure 6b) and the ice clouds (Figure 6c) is less than the total cloud fraction (Figure 6a). In other words, the CALIPSO cloud phase algorithm failed to classify the phase of a large fraction of the CALIPSO-detected clouds in the observations. The fraction of unclassified clouds is greater in the CALIPSO observations than in CAM5. A smaller amount of unclassified clouds in CAM5 is consistent with CAM5 Greenland clouds being optically thinner than observed Greenland clouds.

Previous work shows that liquid-containing clouds strongly influence cloud optical depth and surface radiative fluxes over Greenland [*Miller et al.*, 2015; *Van Tricht et al.*, 2016]. The comparisons shown in Figure 6 suggest that CAM5 underestimates both cloud amount and cloud optical depth. Thus, we next compare CAM5 to ground-based observations to more fully document CAM5 liquid cloud biases and their climate impacts. Table 3 compares cloud liquid water path at Summit, Greenland, in CAM5 and in retrievals [*Turner et al.*, 2007] based on microwave radiometer observations collected as a part of the Integrated Characterization of Energy, Clouds, Atmospheric state, and Precipitation at Summit project [*Shupe et al.*, 2013]. CAM5 liquid water paths are often less than 1% of the observed liquid water paths. In summary, the ground-based liquid water path comparisons are consistent with the spaceborne lidar liquid cloud fraction comparisons: CAM5 has insufficient supercooled liquid cloud. Consistent with insufficient supercooled cloud liquid leading to insufficient downwelling longwave radiation, maximum daily CAM5 2 m air temperatures are on average 2°C lower than observed values (Figure 7).

Table 3. Monthly Mean All-Sky Cloud Liquid Water Path (LWP; g/m2) at Summit, Greenland, from 3 Years of ICECAPS Observations [*Turner et al.*, 2007; *Shupe et al.*, 2013] and CAM5 (Table 1)

	Observed LWP (gm^{-2})	CAM5 LWP/Observed LWP (Percent)
January	4.3	0.0%
February	2.5	0.0%
March	2.4	0.0%
April	1.5	0.2%
May	3.8	0.1%
June	12.2	0.4%
July	25.4	1.2%
August	22.3	0.9%
September	13.1	0.6%
October	6.8	0.2%
November	5.0	0.1%
December	4.2	0.0%
Annual	8.6	0.3%

Moreover, the CAM5 elevation at Summit, Greenland, is ~135 m too low. As a result, the CAM5 cold bias is likely closer to 3°C (assuming lapse rate of 7.1 K/km from *Bennartz et al.* [2013]).

3.3. Regional Evaluation of Southern Hemisphere

We start our evaluation of southern hemisphere extratropical clouds by presenting maps of CALIPSO-observed total cloud cover spatial distributions (Figure 8). The maps reveal that in all seasons, the Southern Ocean (40–70°S) has very large cloud cover (>90%) and the Antarctic continent has much smaller cloud cover (<50%). The observed seasonality in total cloud cover is much smaller over the South Pole/the Antarctic continent (always <35%; Figures 8a–8d) than it is over the North Pole/Arctic Ocean (ranging from 50 to 90%; Figures 3a–3d). CAM5 is able to replicate the large cloud cover over the Southern Ocean and smaller cloud cover over the Antarctic continent, but CAM5 has insufficient clouds in both regions when compared to the observations (Figure 8). When compared to CALIPSO observations, CAM5 has insufficient cloud cover close to the Antarctic continent and also from 30 to 40°S (Table 2).

We next evaluate seasonal maps of southern hemisphere cloud phase biases (Figure 9). Similar to the North Atlantic storm track in DJF, MAM, and SON (Figure 4), CAM5 has excessive Southern Ocean ice cloud in all seasons. CAM5 also has insufficient Southern Ocean liquid clouds in the nonsummer seasons for the southern hemisphere (MAM, JJA, and SON). Over Antarctica, CAM5 has insufficient ice cloud cover in all seasons, especially in JJA and SON. Similar to Greenland in northern hemisphere summer (JJA in Figure 6 and Table 2), the Antarctic continent has insufficient liquid cloud cover in southern hemisphere summer (DJF).

Intrigued by large CAM5 Southern Ocean cloud phase biases (Figure 9), we next examine the seasonal cycle of monthly total, liquid, ice cloud cover (Figure 10). Despite large seasonal differences in temperature and aerosol loading [e.g., *McCoy et al.*, 2015], CALIPSO observations show that Southern Ocean cloud cover remains very constant through the seasonal cycle. At all times of the year over the Southern Ocean, observed low (total) ice cloud fractions are ~4% (~20%), while low (total) liquid cloud cover are ~41% (~47%). When compared to the observations, CAM5 has a larger-than-observed seasonal cycle in ice and liquid cloud cover over the Southern Ocean. As a result, CAM5 has cloud phase biases that are a strong function of season, maximizing in southern hemisphere winter (JJA). These comparisons suggest that the CAM5 physics predicting cloud phase over the Southern Ocean depend too strongly on temperature.

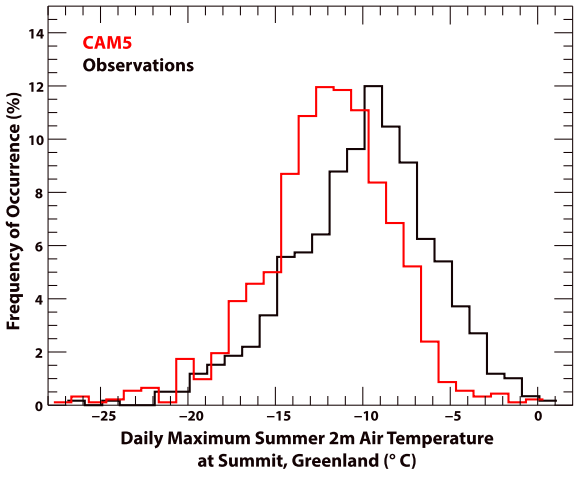

Figure 7. Histogram of daily maximum summer (JJA) 2 m air temperature (units °C) at Summit, Greenland, in CAM5 and observations. Observations from the Global Monitoring Division at the National Oceanic and Atmospheric Administration (http://www.esrl.noaa.gov/gmd/dv/ftpdata.html) are shown for the summers from July 2008 to August 2014.

3.4. Evaluation of Modified Parameterizations to Improve Cloud Phase in CAM5

A large, long-standing, and ubiquitous climate model bias is excessive absorption

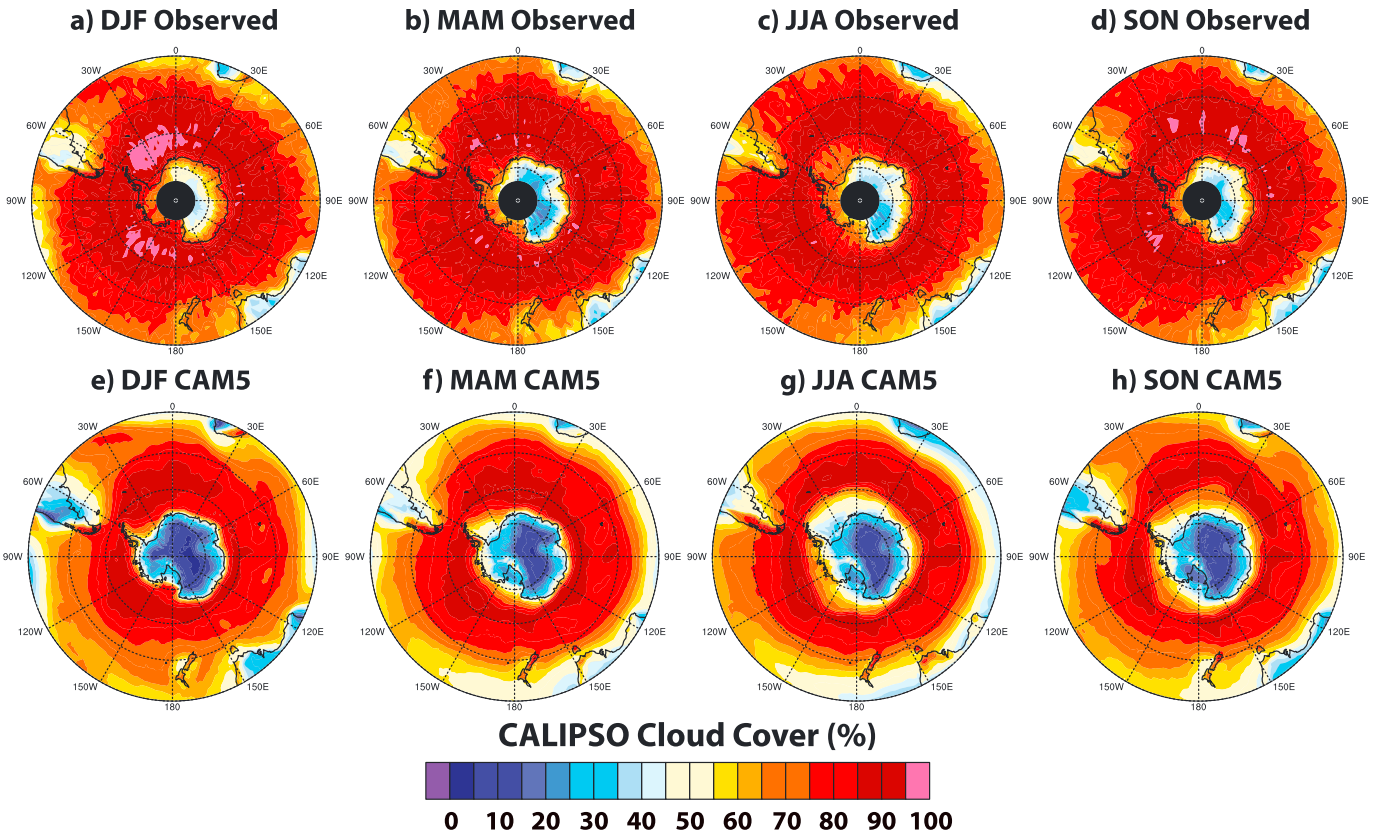

Figure 8. South Pole maps (30–90°S) of total CALIOP cloud cover (units %) by season: (a) observed DJF, (b) observed MAM, (c) observed JJA, and (d) observed SON. (e–h) Same as in Figures 8a–8d but for CAM5.

of shortwave radiation over the Southern Ocean [*Trenberth and Fasullo*, 2010; *Flato et al*., 2013]. This bias is present in almost all CMIP5 models [*Flato et al*., 2013], including CESM-CAM5 [*Kay et al*., 2014]. In an attempt to reduce this large shortwave radiation Southern Ocean bias in CESM-CAM5, we propose a parameter change for the condensate detrainment within the CAM5 shallow convection parameterization (see supporting information). The proposed parameter change enabled condensate formed by shallow convection to be entirely supercooled liquid at temperatures below −5°C. Implementation of this shallow convection parameter change required additional tuning to obtain top-of-atmosphere energy balance and a stable coupled climate. For the rest of the paper, we will use CAM5* as a shorthand for CAM5 simulations with the modifications described in the supporting information. With the exception of the modifications described in the supporting information, the CAM5 and CAM5* runs are identical (Table 1). Here we use the CALIPSO cloud phase diagnostics and Clouds and the Earth's Radiant Energy System–Energy Balanced and Filled (CERES-EBAF) v2.8 2000–2013 [*Loeb et al*., 2009] to contrast cloud phase biases in CAM5 and CAM5* and their corresponding top-of-atmosphere (TOA) shortwave radiation biases.

Figure 11 shows global maps of cloud cover biases in CAM5 and CAM5*. CAM5* has more liquid clouds (+0.8%) and fewer ice clouds (−1.0%) than CAM5. As a result, CAM5* has smaller global mean liquid and ice cloud cover biases than CAM5 when compared to CALIPSO observations. Interestingly, the global annual total cloud cover is a better match to CALIPSO total cloud cover in CAM5 than it is in CAM5*. Increases in the undefined cloud cover bias in CAM5* as compared to CAM5 (not shown) underlie these total cloud cover biases.

Do the changes in cloud cover bias from CAM5 to CAM5* shown in Figure 11 impact TOA radiation? To address this question, we next compare zonal annual mean cloud cover and TOA net shortwave radiation in CAM5 and CAM5* (Figure 12 and Table 4). Over the Southern Ocean where CAM5* has more liquid clouds and fewer ice clouds than CAM5, net TOA shortwave radiation biases are also reduced from 9.0 Wm^{-2} to 0.9 Wm^{-2}. In other words, using CAM5* results in improvements to both the cloud phase biases and the shortwave radiation biases. While the results over the Southern Ocean suggest improvements to climate model liquid and ice cloud cover

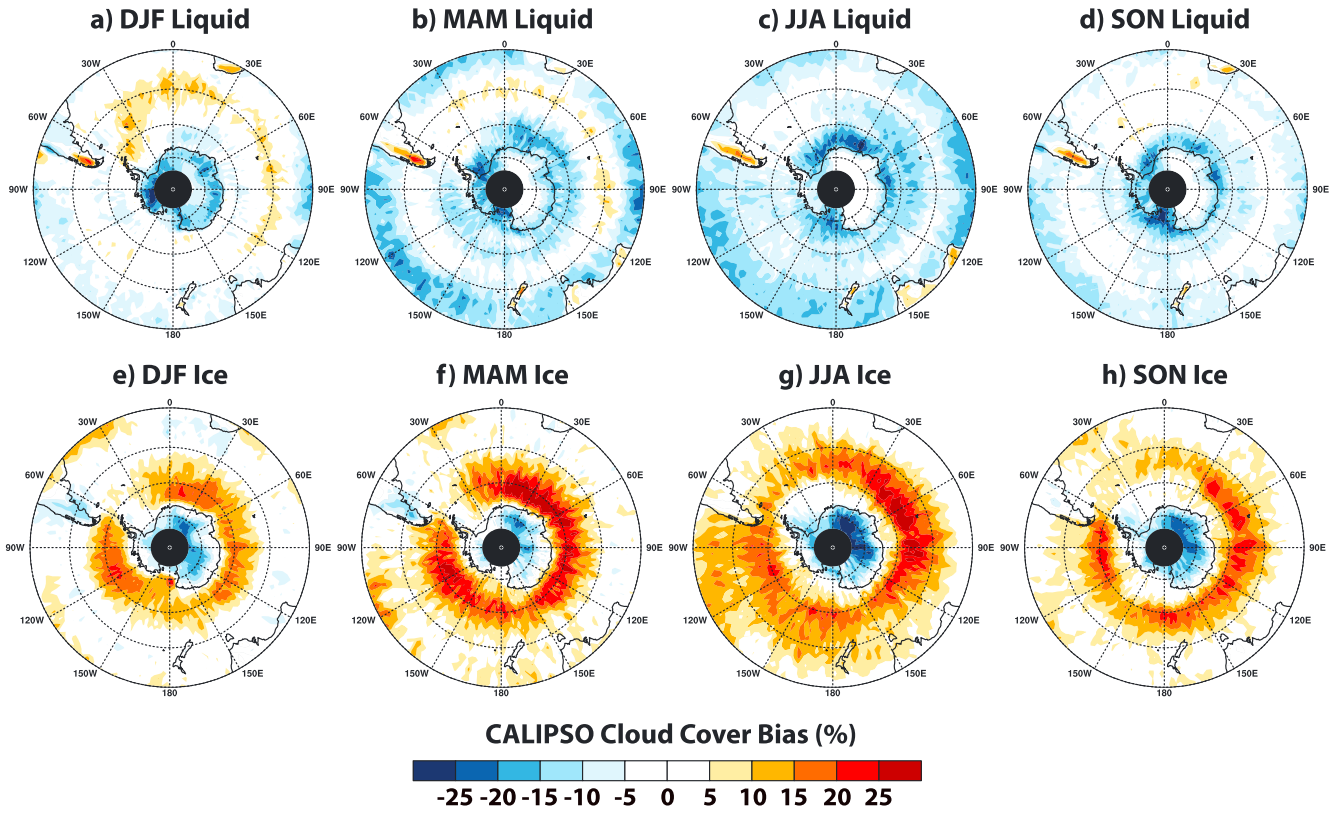

Figure 9. South Pole maps (30–90°S) of CAM5 CALIPSO cloud cover bias (simulated − observed, units %) by season: (a) DJF liquid, (b) MAM liquid, (c) JJA liquid, and (d) SON liquid. (e–h) Same as in Figures 9a–9d but for ice.

biases can lead to large reductions in radiation biases, this result is not universal. Over the tropics, CAM5* has larger cloud cover biases than CAM5, yet CAM5* has smaller shortwave radiation biases than CAM5. Because cloud properties have a substantial influence on cloud radiative impacts, the lack of a universal correspondence between cloud cover changes and shortwave radiation changes is not surprising.

4. Discussion

Combining spaceborne lidar observations of cloud cover, cloud vertical structure, and cloud phase with a lidar satellite simulator provides a powerful constraint on cloud processes in global climate models used

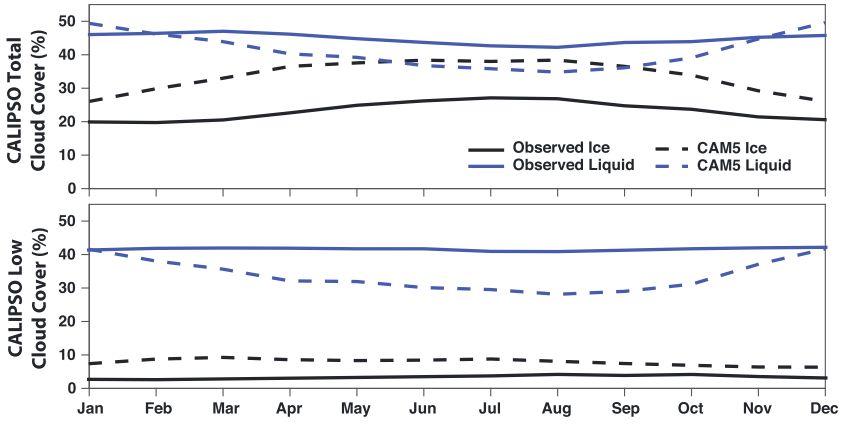

Figure 10. Observed and simulated seasonal cycles of CALIPSO total and low (pressure >680 mb) cloud cover (units %) over the southern hemisphere midlatitude storm track (40–70°S).

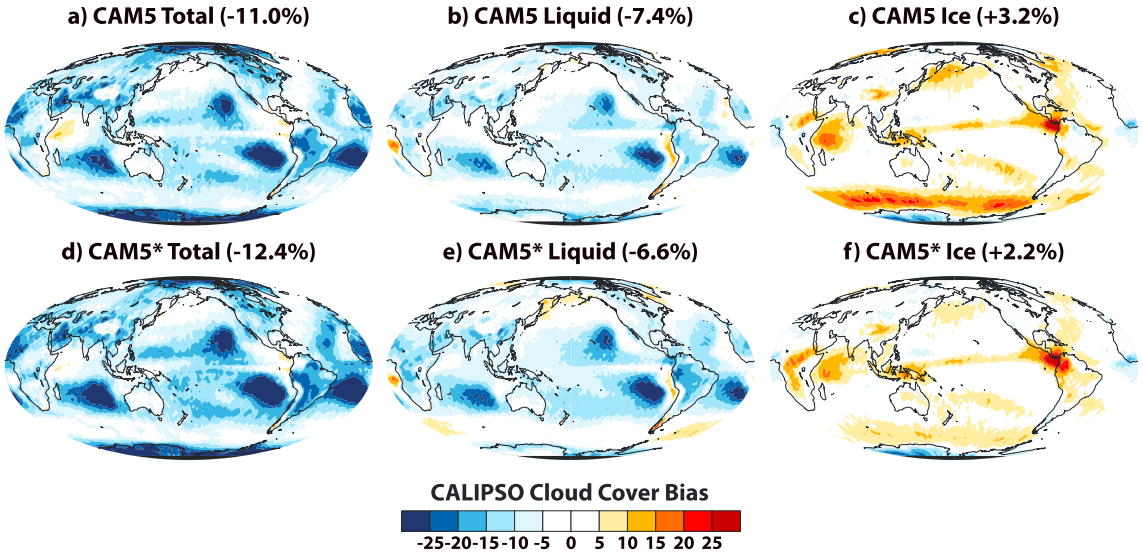

Figure 11. Global maps of CALIPSO cloud cover bias (simulated − observed, units %): (a) CAM5 total, (b) CAM5 liquid, and (c) CAM5 ice. (d–f) Same as in Figures 11a–11c but for CAM5* (CAM5 + modifications to shallow convection; see supporting information).

for future climate projection. The exposition of cloud cover and phase biases in CAM5 in this study raises concerns of global relevance. Beyond CAM5, cloud phase and radiation biases identified in this study are critical to address in future climate model development. For example, the CAM5 cold surface bias over Greenland during northern hemisphere summer (Figure 7) is consistent with insufficient cloud liquid (Figure 6 and Table 2) and may severely limit the utility of coupling ice sheet models with global climate models [e.g., *Vizcaino et al.*, 2015; *Vizcaino*, 2014]. Simply put, we are observing Greenland melting and want to use coupled climate models to provide projections of future melting. Yet if the modeled maximum daily summer temperatures are too cold by 2 to 3°C, as is the case with CAM5, the surface melt extent will be underestimated, and thus, future climate projections of global sea level will be compromised. Another example of a profoundly important cloud bias identified in this study is over the Southern Ocean. Our results indicate that Southern Ocean seasonal variations in cloud phase are too large in CAM5. Larger-than-observed seasonality is concerning because it suggests a stronger temperature dependence in the model than in observations. Indeed, our evaluation suggests that CAM5-simulated warming over the Southern Ocean will likely be accompanied by too large of a phase change from ice to liquid.

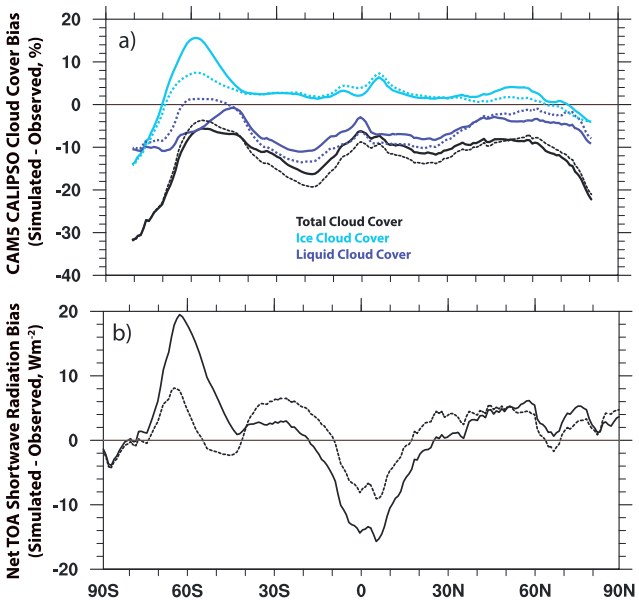

Figure 12. Annual zonal annual mean CAM5 (solid) and CAM5* (dashed) biases (simulated − observed): (a) CALIPSO cloud cover biases (units %) and (b) net top-of-atmosphere (TOA) shortwave radiation bias (units Wm^{-2}) compared to CERES-EBAF v2.8 [*Loeb et al.*, 2009]. CAM5* is CAM5 with modifications to shallow convection (see supporting information).

An overarching result is that geographic or seasonal separation is not nearly as powerful as regime-dependent separation. For example, using "Arctic clouds," typically defined as the average cloud cover from 70–90°N, mixed together biases with origins from multiple climate

Table 4. Zonal Annual Mean Bias in Cloud Cover (CC; Units %) and Top-of-Atmosphere Absorbed Shortwave Radiation (ASR; Units Wm^{-2}) for CAM5 (CAM5-Observed) and CAM5* (CAM5*-Observed)[a]

	Liquid CC CAM5 Bias (%)	Liquid CC CAM5* Bias (%)	Ice CC CAM5 Bias (%)	Ice CC CAM5* Bias (%)	ASR CAM5 Bias (Wm^{-2})	ASR CAM5* Bias (Wm^{-2})
70–82 N	−6	−4	−1	−3	4	2
60–70 N	−4	−2	2	−0	2	−0
50–60 N	−4	−2	4	1	5	4
40–50 N	−3	−3	3	1	4	5
30–40 N	−6	−7	2	1	2	4
20–30 N	−8	−10	2	2	−1	3
10–20 N	−7	−10	3	3	−6	−2
0–10 N	−6	−9	5	6	−14	−7
0–10 S	−6	−9	3	4	−11	−5
10–20 S	−10	−12	2	2	−2	3
20–30 S	−10	−13	3	2	2	6
30–40 S	−8	−9	3	2	3	5
40–50 S	−2	−2	5	3	3	−2
50–60 S	−5	1	14	6	12	0
60–70 S	−9	−3	10	4	16	6
70–82 S	−10	−9	−7	−8	2	0
Global	−7	−7	4	2	0	1

[a]Observations are from the CALIPSO GOCCP product version 2.8 [*Chepfer et al*., 2010; *Cesana and Chepfer*, 2013] and CERES-EBAF version 2.8 [*Loeb et al*., 2009]. See Table 1 for CAM5 and CAM5* description.

regions (storm tracks, ice-covered Arctic Ocean, and newly open water Arctic Ocean). Indeed, identifying the specific cloud regime (postfrontal shallow convection in midlatitude cyclones [see *Bodas-Salcedo et al*., 2014] is essential to the cloud phase and shortwave radiation bias reductions accomplished by modifying the shallow convection (see Figures 11 and 12).

5. Summary

This study uses spaceborne lidar observations to evaluate cloud phase biases in the atmospheric component (CAM5) of a widely used global climate model (CESM). Importantly, the idiosyncrasies of spaceborne lidar cloud detection and phase assignment are replicated within the model providing scale-aware and definition-aware comparisons. When compared to the observations, CAM5 has insufficient liquid cloud and excessive ice cloud in most regions. Over the ice-covered Arctic Ocean, CAM5 has insufficient liquid cloud in all seasons. A summertime liquid cloud deficit contributes to a cold bias of 2 to 3°C for daily maximum near-surface air temperatures at Summit, Greenland. Over the midlatitude storm tracks, CAM5 has excessive ice cloud and insufficient liquid cloud. CAM5 storm track cloud phase biases maximize over the Southern Ocean, which also has larger-than-observed seasonal variations in cloud phase. Modifications to the shallow convective detrainment reduce Southern Ocean cloud phase and shortwave radiation biases, providing an illustrative example of the power of the satellite-observed cloud phase constraint in a climate modeling context.

More generally, this study shows the value of spaceborne lidar observations and lidar simulators. Easily available and directly comparable observations are needed to benchmark and improve climate models. CALIPSO observations can be used to evaluate next-generation development of climate models in a simulator framework, e.g., for the next Coupled Model Intercomparison Project 6 (CMIP6) [*Meehl et al*., 2014]. Although the improvement of global climate models can be daunting, it is especially encouraging to see that simple parameter changes such as those shown for CAM5* in this work (Table 1) can lead to such large reductions in cloud phase and radiation flux biases over the Southern Ocean. Climate modeling centers are improving cloud and precipitation processes including prognostic precipitation and substepping of microphysical/macrophysical processes [e.g., *Gettelman et al*., 2015]. What is the impact of these changes on cloud phase biases evaluated within a scale-aware and definition-aware framework? When combined with spaceborne lidar observations, satellite simulators are an invaluable asset to evaluate clouds in climate models used for future climate projection.

Acknowledgments
The authors wish to thank the Yellowstone CESM CSL for computing the resources and the scientists and software engineers that build the CESM. This work was funded by NASA 12-CCST10-0095. The National Center for Atmospheric Research is sponsored by the National Science Foundation. The source code for the model used in this study, the Community Earth System Model (CESM) version 5, is freely available at http://www2.cesm.ucar.edu/. The data have been archived on the NCAR High Performance Storage System Repository at /home/jenkay/cosp/production_runs/runs_cam5_3_88.

References

Bennartz, R., M. D. Shupe, D. D. Turner, V. P. Walden, K. Steffen, C. J. Cox, M. S. Kulie, N. B. Miller, and C. Pettersen (2013), July 2012 Greenland melt extent enhanced by low-level liquid clouds, *Nature*, *496*, 83–86, doi:10.1038/nature12002.

Bodas-Salcedo, A., et al. (2011), COSP: Satellite simulation software for model assessment, *Bull. Am. Meteorol. Soc.*, *92*, 1023–1043.

Bodas-Salcedo, A., K. D. Williams, M. A. Ringer, I. Beau, J. N. S. Cole, J.-L. Dufresne, T. Koshiro, B. Stevens, Z. Wang, and T. Yokohata (2014), Origins of solar radiation biases over the Southern Ocean in CFMIP2 models, *J. Clim.*, *27*, 41–56, doi:10.1175/JCLI-D-13-00169.1.

Cesana G., and H. Chepfer (2012), How well do climate models simulate cloud vertical structure? A comparison between CALIPSO-GOCCP satellite observations and CMIP5 models, *Geophys. Res. Let.*, *39*, L20803, doi:10.1029/2012GL053153.

Cesana, G., and H. Chepfer (2013), Evaluation of the cloud thermodynamic phase in a climate model using CALIPSO-GOCCP, *J. Geophys. Res. Atmos.*, *118*, 7922–7937, doi:10.1002/jgrd.50376.

Cesana, G., J. E. Kay, H. Chepfer, J. M. English, and G. de Boer (2012), Ubiquitous low-level liquid-containing Arctic clouds: New observations and climate model constraints from CALIPSO-GOCCP, *Geophys. Res. Lett.*, *39*, L20804, doi:10.1029/2012GL053385.

Chepfer, H., S. Bony, D. M. Winker, M. Chiriaco, J.-L. Dufresne, and G. Seze (2008), Use of CALIPSO lidar observations to evaluate the cloudiness simulated by a climate model, *Geophys. Res. Lett.*, *35*, L15704, doi:10.1029/2008GL034207.

Chepfer H., S. Bony, D. Winker, G. Cesana, J. L. Dufresne, P. Minnis, C. J. Stubenrauch, and S. Zeng (2010), The GCM Oriented CALIPSO Cloud Product (CALIPSO-GOCCP), *J. Geophys. Res.*, *115*, D00H16, doi:10.1029/2009JD012251.

Chepfer, H., G. Cesana, D. Winker, B. Getzewich, M. Vaughan, and Z. Liu (2013), Comparison of two different cloud climatologies derived from CALIOP level 1 observations: The CALIPSO-ST and the CALIPSO-GOCCP, *J. Atmos. Oceanic Technol.*, doi:10.1175/JTECH-D-12-00057.1.

Dee, D. P., et al. (2011), The ERA-Interim reanalysis: Configuration and performance of the data assimilation system, *Q. J. R. Meteorol. Soc.*, *137*, 553–597, doi:10.1002/qj.828.

English, J. M., J. E. Kay, A. Gettelman, X. Liu, Y. Wang, Y. Zhang, and H. Chepfer (2014), Contributions of clouds, surface albedos, and mixed-phase ice nucleation schemes to Arctic radiation biases in CAM5, *J. Clim.*, doi:10.1175/JCLI-D-13-00608.1.

Flato, G., et al. (2013), Evaluation of climate models, in *Climate Change 2013: The Physical Science Basis. Contribution of Working Group I to the Fifth Assessment Report of the Intergovernmental Panel on Climate Change*, edited by T. F. Stocker et al., Cambridge Univ. Press, Cambridge, U. K., and New York.

Forbes, R. M., and M. Ahlgrimm (2014), On the representation of high-latitude boundary layer mixed-phase cloud in the ECMWF global model, *Mon. Weather Rev.*, *142*, 3425–3445, doi:10.1175/MWR-D-13-00325.1.

Frölicher, T. L., J. L. Sarmiento, D. J. Paynter, J. P. Dunne, J. P. Krasting, and M. Winton (2015), Dominance of the Southern Ocean in anthropogenic carbon and heat uptake in CMIP5 models, *J. Clim.*, *28*, 862–886, doi:10.1175/JCLI-D-14-00117.1.

Gettelman, A., H. Morrison, S. Santos, P. Bogenschutz, and P. M. Caldwell (2015), Advanced two-moment bulk microphysics for global models. Part II: Global model solutions and aerosol–cloud interactions, *J. Clim.*, *28*, 1288–1307, doi:10.1175/JCLI-D-14-00103.1.

Hurrell, J., et al. (2013), The Community Earth System Model: A framework for collaborative research, *Bull. Am. Meteorol. Soc.*, doi:10.1175/BAMS-D-12-00121.1.

Hu, Y., S. Rodier, K. Xu, W. Sun, J. Huang, B. Lin, P. Zhai, and D. Josset (2010), Occurrence, liquid water content, and fraction of supercooled water clouds from combined CALIOP/IIR/MODIS measurements, *J. Geophys. Res.*, *115*, D00H34, doi:10.1029/2009JD012384.

Hwang, Y.-T., and D. M. W. Frierson (2013), A link between the double Intertropical Convergence Zone problem and cloud biases over the Southern Ocean, *Proc. Natl. Acad. Sci. U.S.A*, doi:10.1073/pnas.1213302110.

Kay, J. E., T. L'Ecuyer, A. Gettelman, G. Stephens, and C. O'Dell (2008), The contribution of cloud and radiation anomalies to the 2007 Arctic sea ice extent minimum, *Geophys. Res. Lett.*, *35*, L08503, doi:10.1029/2008GL033451.

Kay, J. E., et al. (2012), Exposing global cloud biases in the Community Atmosphere Model (CAM) using satellite observations and their corresponding instrument simulators, *J. Clim.*, *25*, 5190–5207, doi:10.1175/JCLI-D-11-00469.1.

Kay, J. E., B. Medeiros, Y.-T. Hwang, A. Gettelman, J. Perket, and M. G. Flanner (2014), Processes controlling Southern Ocean shortwave climate feedbacks in CESM, *Geophys. Res. Lett.*, *41*, 616–622, doi:10.1002/2013GL058315.

Kay, J. E., et al. (2015), The Community Earth System Model (CESM) large ensemble project: A community resource for studying climate change in the presence of internal climate variability, *Bull. Am. Meteorol. Soc.*, *96*, 1333–1349, doi:10.1175/BAMS-D-13-00255.1.

Kay, J. E., C. J. Wall, V. Yettella, B. Medeiros, C. Hannay, P. Caldwell, and C. Bitz (2016), Global climate impacts of fixing the Southern Ocean shortwave radiation bias in the Community Earth System Model, *J. Clim.*, doi:10.1175/JCLI-D-15-0358.1, in press.

Loeb, N. G., et al. (2009), Toward optimal closure of the earth's top-of-atmosphere radiation budget, *J. Clim.*, *22*, 748–766, doi:10.1175/2008JCLI2637.1.

McCoy, D. T., S. M. Burrows, R. Wood, D. P. Grosvenor, S. M. Elliott, P.-L. Ma, P. J. Rasch, and D. L. Hartmann (2015), Natural aerosols explain seasonal and spatial patterns of Southern Ocean Cloud albedo, *Sci. Adv.*, doi:10.1126/scoadv.1500157.

Meehl, G. A., R. Moss, K. E. Taylor, V. Eyring, R. J. Stouffer, S. Bony, and B. Stevens (2014), Climate model intercomparisons: Preparing for the next phase, *Eos Trans. AGU*, *95*(9), 77, doi:10.1002/2014EO090001.

Mikaloff-Fletcher, S. E. (2015), An increasing carbon sink?, *Science*, *349*(6253), 1165, doi:10.1126/science.aad0912.

Miller, N., M. Shupe, C. Cox, V. Walden, D. Turner, and K. Steffen (2015), Cloud radiative forcing at Summit, Greenland, *J. Clim.*, *28*, 6267–6280, doi:10.1175/JCLI-D-15-0076.1.

Morrison, H., G. de Boer, G. Feingold, J. Harrington, M. D. Shupe, and K. Sulia (2012), Resilience of persistent Arctic mixed-phase clouds, *Nat. Geosci.*, *5*, 11–17, doi:10.1038/ngeo1332.

Nam C., S. Bony, J. L. Dufresne, and H. Chepfer (2012), The "too few, too bright" tropical low-cloud problem in CMIP5 models, *Geophys. Res. Lett.*, *39*, L21801, doi:10.1029/2012GL053421.

Neale, R. B., et al. (2012), Description of the NCAR Community Atmosphere Model (CAM5), Technical Report NCAR/TN-486+STR, National Center for Atmospheric Research, Boulder, Colorado, 268 pp.

Shepherd, A., et al. (2012), A reconciled estimate of ice-sheet mass balance, *Science*, *338*, 1183–1189, doi:10.1126/science.1228102.

Shupe, M. D., and J. M. Intrieri (2004), Cloud radiative forcing of the Arctic surface: The influence of cloud properties, surface albedo, and solar zenith angle, *J. Clim.*, *17*, 616–628, doi:10.1175/1520-0442(2004)017<0616:CRFOTA>2.0.CO;2.

Shupe, M. D., et al. (2013), High and dry: New observations of tropospheric and cloud properties above the Greenland Ice Sheet, *Bull. Am. Meteorol. Soc.*, *94*, 169–186, doi:10.1175/BAMS-D-11-00249.1.

Stroeve, J. C., M. C. Serreze, M. M. Holland, J. E. Kay, W. Meier, and A. P. Barrett (2012), The Arctic's rapidly shrinking sea ice cover: A research synthesis, *Clim. Change*, *110*, 3–4, 1005–1027, doi:10.1007/s10584-011-0101-1.

Stubenrauch, C. J., et al. (2013), Assessment of global cloud datasets from satellites: Project and database initiated by the GEWEX radiation panel, *Bull. Am. Meteorol. Soc.*, *94*, 1031–1049, doi:10.1175/BAMS-D-12-00117.1.

Taylor, K. E., R. J. Stouffer, and G. A. Meehl (2012), The CMIP5 experiment design, *Bull. Am. Meteorol. Soc.*, *93*, 485–498, doi:10.1175/BAMS-D-11-00094.1.

Trenberth, K. E., and J. T. Fasullo (2010), Simulation of present-day and twenty first-century energy budgets of the southern oceans, *J. Clim.*, *23*, 440–454, doi:10.1175/2009JCLI3152.1.

Turner, D. D., et al. (2007), Retrieving liquid water path and precipitable water vapor from the Atmospheric Radiation Measurement (ARM) microwave radiometers, *IEEE Trans. Geosci. Remote Sens.*, *45*, 11, doi:10.1109/TGRS.2007.903703.

Van Tricht, K., S. Lhermitte, J. T. M. Lenaerts, I. V. Gorodetskaya, T. L'Ecuyer, B. Noel, M. R. van den Broeke, D. D. Turner, and N. P. M. van Lipzig (2016), Clouds enhance Greenland ice sheet meltwater runoff, *Nat. Commun.*, *7*, 10,266, doi:10.1038/ncomms10266.

Vizcaino, M. (2014), Ice sheets as interactive components of Earth System Models: Progress and challenges, *WIREs Clim. Change*, *5*, 557–568, doi:10.1002/wcc.285.

Vizcaino, M., U. Mikolajewicz, F. Ziemen, C. B. Rodehacke, R. Greve, and M. R. van den Broeke (2015), Coupled simulations of Greenland Ice Sheet and climate change up to A.D. 2300, *Geophys. Res. Lett.*, *42*, 3927–3935, doi:10.1002/2014GL061142.

Winker, D. M., et al. (2010), The CALIPSO mission: A global 3D view of aerosols and clouds, *Bull. Am. Meteorol. Soc.*, *91*, 1211–1229, doi:10.1175/2010BAMS3009.1.